I R A M P
13(1), Jan 2022, pp. 27-34

ISSN: 2229-39-44

Classical Stark Effect of Circular Rydberg States of He and He-like Ions

N. KRYUKOV[1] AND E. OKS[2,*]

[1]*Universidad Nacional Autónoma de México, Av. Universidad 3000, col. Ciudad Universitaria, del. Coyoacán, México, DF 04510, Mexico*
[2]*Physics Department, 380 Duncan Drive, Auburn University, Auburn, AL 36849, USA*

ABSTRACT: Circular Rydberg States (CRS) were studied theoretically and experimentally in lots of works. In particular, in the previous paper by one of us, there were derived analytical expressions for the energy of classical CRS in collinear electric (**F**) and magnetic (**B**) fields of arbitrary strengths imposed on a hydrogenic system (atom or ion). In that paper the author provided formulas for the dependence of the classical ionization threshold $F_c(B)$ and of the energy at this threshold $E_c(B)$ valid for the magnetic field **B** of an arbitrary strength. He also analyzed the stability of the motion by going beyond the CRS. In addition, for two important particular cases previously studied in the literature – classical CRS in a magnetic field only and classical CRS in an electric field only – some new results were also presented in that paper, especially concerning the Stark effect. In the present paper we study analytically CRS of a heliumic system (He atom or He-like ion) subjected to an electric field of an arbitrary strength. We show that the difference in the unperturbed structure of the heliumic systems (compared to hydrogenic systems) causes the decrease of the classical ionization threshold, as well as increases the energy and the orbit radius at the ionization threshold. Also, the allowance for the non-zero size of the internal subsystem increases the maximum possible absolute value of the induced electric dipole moment.

Keywords: circular Rydberg states; He and He-like ions; classical Stark effect

1. INTRODUCTION

Circular Rydberg States (CRS) were studied theoretically and experimentally in lots of works – see, e.g., papers [1-10] and references therein. In particular, in paper [11] there were derived analytical expressions for the energy of classical CRS in collinear electric (**F**) and magnetic (**B**) fields of arbitrary strengths imposed on a hydrogenic system (atom or ion). In paper [11] the author provided formulas for the dependence of the classical ionization threshold $F_c(B)$ and of the energy at this threshold $E_c(B)$ valid for the magnetic field **B** of an arbitrary strength. He also analyzed the stability of the motion by going beyond the CRS. In addition, for two important particular cases previously studied in the literature – classical CRS in a magnetic field only [9] and classical CRS in an electric field only [10] – some new results were also presented in paper [11].

In the present paper we study analytically CRS of a heliumic system (He atom or He-like ion) subjected to an electric field of an arbitrary strength. We show that the difference in the unperturbed structure of the heliumic systems (compared to hydrogenic systems) causes the decrease of the classical ionization threshold, as well as increases the energy and the orbit radius at the ionization threshold.

2. RESULTS

We consider a He atom or a He-like atom/ion, where the electrons are in circular Rydberg states, the orbits are concentric and coplanar, and the classical orbit radius of one electron is significantly different from that of the other. This system is placed into an electric field **F** parallel to the axis of the orbits.

The revolution frequency of the inner system "$Zp^+ – e^-$" is

$$\omega_{\text{int}} = \sqrt{\frac{Ze^2}{\bar{m}r^3}} \tag{1}$$

where Z is the nuclear charge, e is the electron charge, r is the distance between the nucleus and the inner electron and $\bar{m}$ is their reduced mass:

$$\bar{m} = \frac{Mm}{M+m} \tag{2}$$

where M is the nuclear mass and m is the electron mass. The radii of rotation of the nucleus and the inner electron are

$$r_1 = \frac{m}{M+m}r, \qquad r_2 = \frac{M}{M+m}r \tag{3}$$

The revolution frequency of the outer system "(Zp^+ and e^-) – e^-" is

$$\omega_{ext} = \sqrt{\frac{(Z-1)e^2}{\bar{m}'R^3}} \tag{4}$$

where R is the distance from the center of the inner system to the outer electron and $\bar{m}'$ is the reduced mass of the outer system:

$$\bar{m}' = \frac{(M+m)m}{M+2m} \tag{5}$$

As $R >> r$ by the original statement, $\omega_{ext} << \omega_{int}$, which means that the inner system represents the rapid subsystem and the outer system represents the slow subsystem. Therefore, the outer electron perceives the nucleus and the inner electron as charged circular rings of radii r_1 and r_2 with the charge distributed uniformly around each ring.

The primary potential term for the outer electron is the Coulomb monopole interaction with the inner system:

$$U_0 = -\frac{Z-1}{R} \tag{6}$$

The quardupole interaction terms of the outer electron with the nuclear and electronic rings are (see, e.g., [12, 13])

$$U_1^{(1)} = -Ze^2r_1^2\frac{3\cos^2\theta - 1}{4R^3}, \qquad U_1^{(2)} = -e^2r_2^2\frac{3\cos^2\theta - 1}{4R^3} \tag{7}$$

where θ is the spherical polar angle, so the total quadrupole interaction is found by adding both and utilizing (3):

$$U_1 = -\frac{(Zm^2+M^2)e^2r^2}{(M+m)^2}\frac{3\cos^2\theta - 1}{4R^3} \tag{8}$$

We will use atomic units, where $m = e = 1$. Thus, the Hamiltonian of the outer electron, on which we will concentrate our analysis, is

$$H = \frac{L^2}{2\rho^2} - \frac{Z-1}{R} - \frac{(Z+M^2)r^2}{(M+1)^2}\frac{3\cos^2\theta - 1}{4R^3} + Fz \tag{9}$$

where L is the angular momentum and (ρ, φ, z) are the cylindrical coordinates of the outer electron. Because $M >> 1$, the quadrupole term can be approximated further:

$$H = \frac{L^2}{2\rho^2} - \frac{Z-1}{R} - r^2 \frac{3\cos^2\theta - 1}{4R^3} + Fz \tag{10}$$

With $R = (\rho^2 + z^2)^{1/2}$ and the scaled quantities

$$w = \frac{Z-1}{L^2} z, v = \frac{Z-1}{L^2} \rho, p = v^2, f = \frac{L^4}{(Z-1)^3} F, \lambda = \frac{\sqrt{Z-1}}{L^2} r, \varepsilon = \frac{L^2}{(Z-1)^2} H \tag{11}$$

we express the scaled energy of the outer electron in the following form:

$$\varepsilon = \frac{1}{2p} - \frac{1}{\sqrt{w^2+p}} - \frac{\lambda^2}{4} \frac{2w^2 - p}{(w^2+p)^{5/2}} + fw \tag{12}$$

To find the equilibrium, the derivatives of (12) with respect to the scaled coordinates w and p should vanish:

$$\frac{\partial \varepsilon}{\partial w} = 0, \qquad \frac{\partial \varepsilon}{\partial p} = 0 \tag{13}$$

The first equation yields

$$-\frac{f}{w} = \frac{1}{(w^2+p)^{3/2}} + \frac{3\lambda^2}{4} \frac{2w^2 - 3p}{(w^2+p)^{7/2}} \tag{14}$$

and the second one yields

$$\frac{1}{p^2} = \frac{1}{(w^2+p)^{3/2}} + \frac{3\lambda^2}{4} \frac{4w^2 - p}{(w^2+p)^{7/2}} \tag{15}$$

When f increases from 0, the system acquires an induced dipole moment, with $w < 0$ for $f > 0$, so that the orbital plane is shifted along the axis of symmetry in the direction opposite to that of the electric field. Fig. 1 schematically presents this situation for $f > 0$. There are two equilibrium points for an infinitesimal f: the stable one at $w \approx -f$ and the unstable one at infinity.

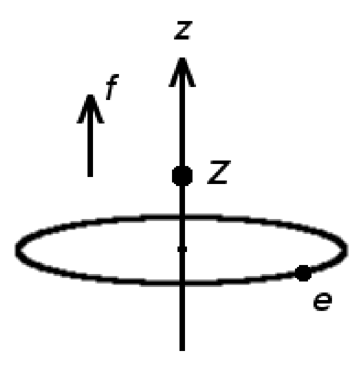

Fig. 1. The shift of the orbital plane of the electron in the presence of the electric field parallel to the axis of symmetry of the orbit. The nucleus of charge Z is at the origin $z = 0$.

Fig. 2 shows the equilibrium points (w, v) satisfying (14) and (15) depending on the electric field increasing from $f = 0.01$ to $f = 0.2$ with $\lambda = 0.05$.

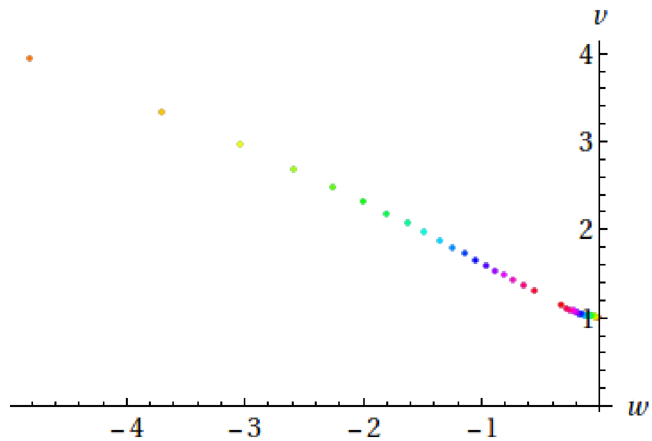

Fig. 2. Equilibrium points in the plane (w, v) depending on the electric field increasing from f = 0.01 to f = 0.2 with λ = 0.05 (the points corresponding to the increasing field are shown with a color gradient, from red to violet).

As expected, we observe here the two equilibria. The set of points on the right (near $w = 0$, $v = 1$) corresponds to the solution of the unperturbed electron in the Coulomb field of the nucleus without the external electric field, modified by the external electric field f and the size of the inner system λ. The set of points on the left (beginning from the top-left point) corresponds to the equilibrium where $|w|$ and v tend to infinity as f tends to zero. We see that the electric field increases the orbit radius and shifts the orbit center down from zero on the z-axis (for $f > 0$) for the zero-w equilibrium, and produces the opposite effect on the infinite-w equilibrium (decreases the orbit radius and brings the center closer to the nucleus).

Fig. 3 shows the equilibrium points (w, v) for the electric field $f = 0.1$ with λ increasing from λ = 0.01 to λ = 0.3.

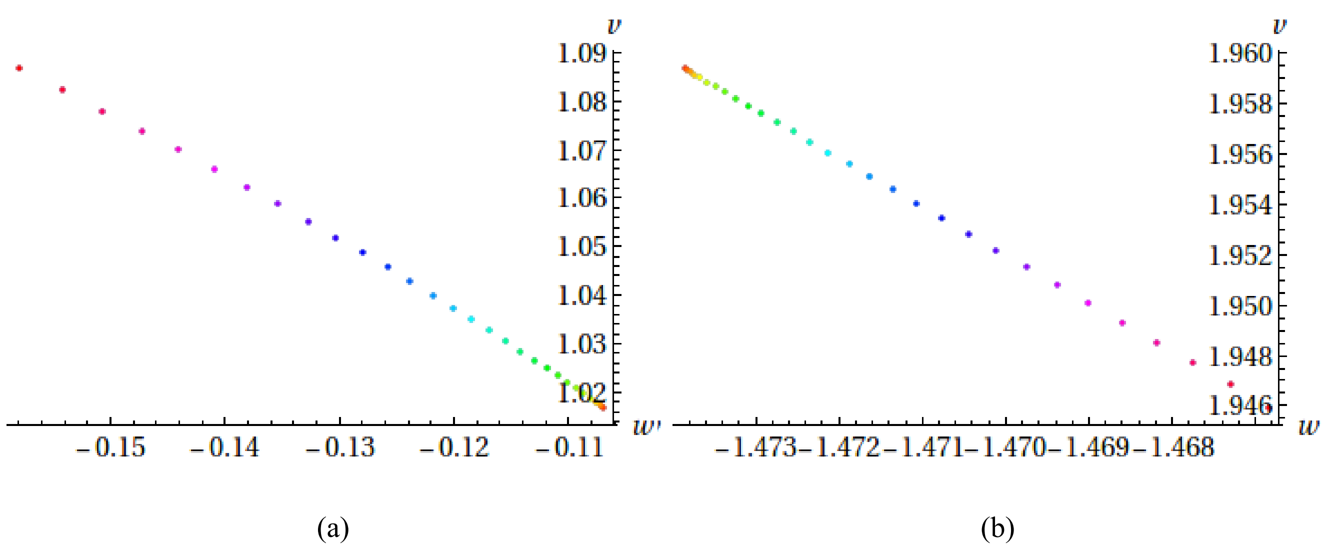

Fig. 3. Equilibrium points in the plane (w, v) depending on the size of the inner system λ from λ = 0.01 to λ = 0.3 (a) for the zero-w (stable) equilibrium and (b) for the infinite-w (unstable) equilibrium (the points corresponding to the increasing λ are shown with a color gradient, from red to violet).

From Fig. 3 we see that the effect of λ on the equilibrium is similar to the effect of the electric field: the non-point-like nature of the inner system increases the orbit radius and shifts the orbit center down from zero on the z-

axis (for $f > 0$) for the zero-w stable equilibrium, and produces the opposite effect on the infinite-w unstable equilibrium.

Fig. 4 shows the dependence of the outer electron's energy on the electric field strength, for the values of $\lambda = 0.1$ and $\lambda = 0.2$.

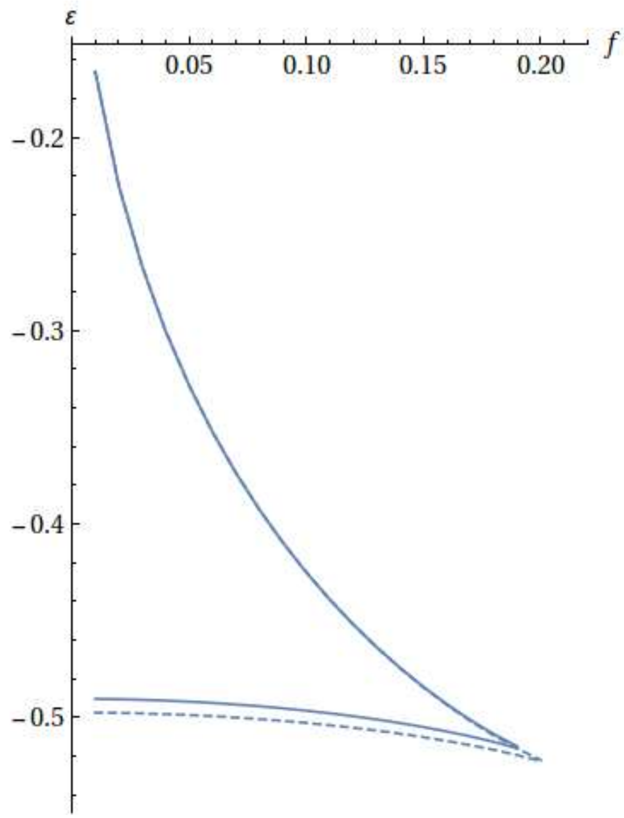

Fig. 4. Dependence of the scaled energy ε of the outer electron on the electric field *f* for λ = 0.1 (dashed curve) and λ = 0.2 (solid curve).

The case of $\lambda = 0$ was studied in paper [11]. As in that case, we observe the existence of an ionization threshold, the point $f = f_c$ and $\varepsilon = \varepsilon_c$ where both equilibria exhibit a V-type crossing. At the crossing, the outer electron switches from the stable equilibrium to the unstable equilibrium, the latter leading to the ionization. From Fig. 4 we see that the non-zero size of the inner system increases the ionization threshold energy and decreases the critical electric field corresponding to the ionization threshold.

To find the ionization threshold, we use the fact that both implicit functions $p(w)$ given by (14) and (15) have the same point (w, p) (the point of equilibrium) and their derivatives are equal because this point is where both curves are tangent to each other – for a lesser field they intersect in two points and for a greater field they have no common points. By differentiating (14) and (15) with respect to w, solving each resulting equation for dp/dw and setting the two solutions equal, we obtain the third equation in addition to (14) and (15), which gives us the set of the quantities (w, p, f) corresponding to the ionization threshold for a given λ.

Fig. 5 shows the dependence of the critical field f_c corresponding to the ionization threshold on the size of the inner system λ.

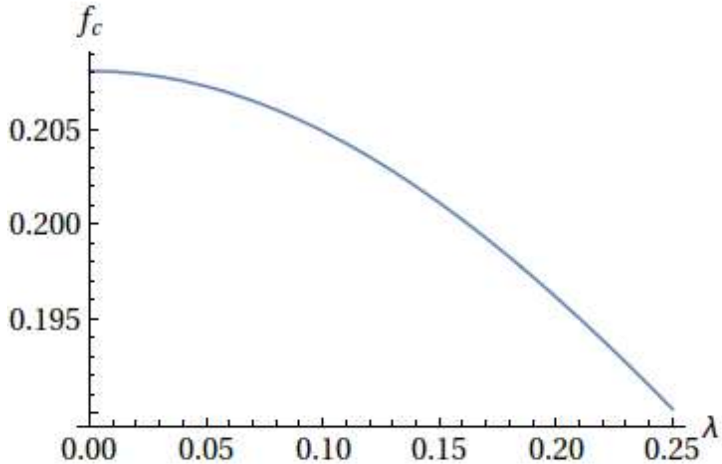

Fig. 5. Dependence of the critical field f_c corresponding to the ionization threshold on the size of the inner system λ.

As we observed earlier, the non-zero λ decreases the critical electric field.

Fig. 6 shows the energy of the outer electron at the ionization threshold.

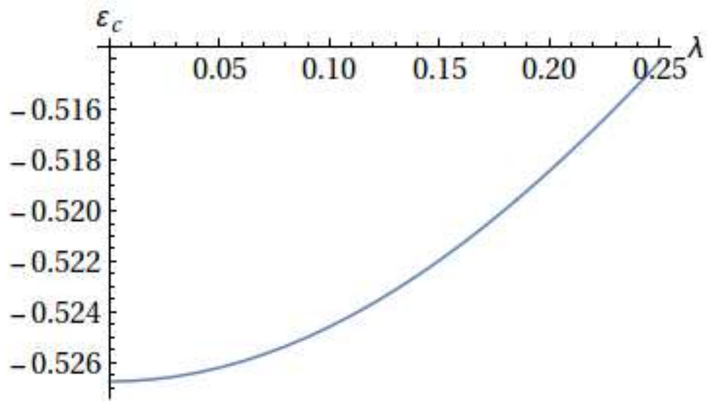

Fig. 6. Dependence of the energy ε_c of the outer electron at the ionization threshold on the size of the inner system λ.

We see that the non-zero size of the inner system increases the energy at the ionization threshold.

For the quadrupole interaction term starting from (7) to be valid, the orbit radius of the outer electron must be much greater than the size of the inner system: $R/r = \eta >> 1$. Using (11), this yields

$$\eta = \frac{\sqrt{w^2 + p}}{\lambda\sqrt{Z-1}} \gg 1 \tag{16}$$

Fig. 7 shows the ratio of the orbit radii depending on f for the case of $\lambda = 0.1$ and on λ for the case of $f = 0.1$.

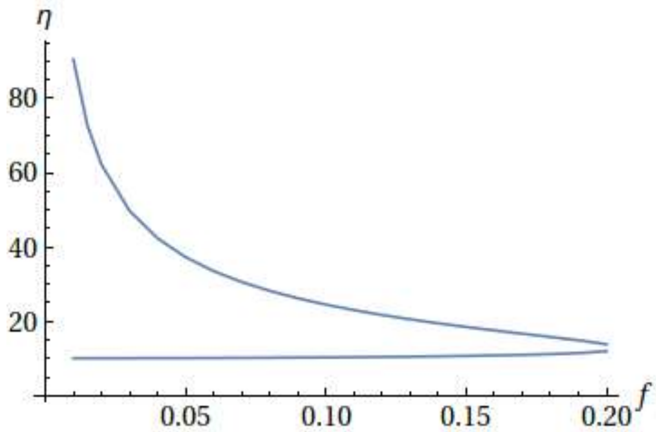

(a)

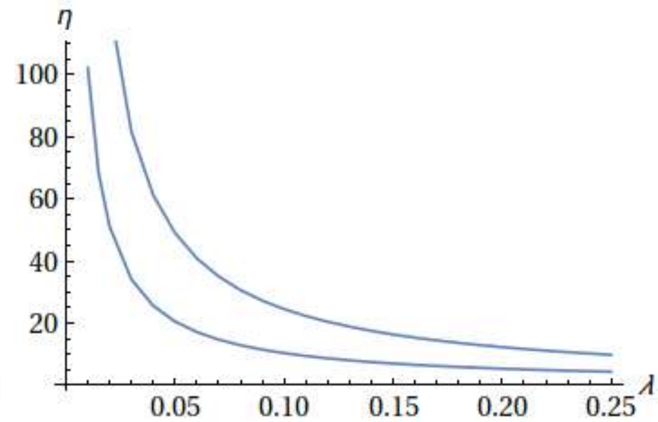

(b)

Fig. 7. Dependence of the ratio of the orbit radius of the outer electron to that of the inner electron (a) on the electric field for scaled size of the inner system λ = 0.1 and (b) on λ for the scaled electric field *f* = 0.1.

From Fig. 7 we see that the ratio is relatively large in the cases considered, which confirms the validity of the analysis. We remind the readers that there are two states of equilibrium of different energies: the lower branch in each plot in Fig. 7 corresponds to the zero-*w* equilibrium, which is stable, and the upper branch corresponds to the infinite-*w* equilibrium, which is unstable. The upper branch, which corresponds to the unstable equilibrium, corresponds also to large orbit radii *R*; therefore, the ratio $\eta = R/r$ is greater than in the case of stable equilibrium, which corresponds to the lower branch in Fig. 7.

We also performed an analytical approximation of the equilibrium shift and orbit radius, the energy, and the ionization threshold, for small values of λ and compared them to the zero-λ values from paper [11]. In the approximation, the subscript "0" refers to the zero-λ values. Equations (17) – (19) show the approximate values of the axial shift, electric field and energy depending on the parameter *p* (squared scaled orbit radius).

$$w \approx -\sqrt{p(p^{1/3}-1)} + \frac{\frac{5}{4p^{1/3}}-1}{\sqrt{p(p^{1/3}-1)}}\lambda^2 = w_0 - \frac{1}{w_0}\left(\frac{5}{4p^{1/3}}-1\right)\lambda^2 \tag{17}$$

$$f \approx \frac{\sqrt{p^{1/3}-1}}{p^{3/2}} - \frac{2p^{1/3}-1}{4p^{17/6}\sqrt{p^{1/3}-1}} = f_0 - \frac{1}{4p^4 f_0}\left(2-\frac{1}{p^{1/3}}\right)\lambda^2 \tag{18}$$

$$\varepsilon \approx \frac{3}{2p} - \frac{2}{p^{2/3}} + \frac{\lambda^2}{2p^{7/3}} = \varepsilon_0 + \frac{\lambda^2}{2p^{7/3}} \tag{19}$$

Equations (20) – (23) show the approximate values of the ionization threshold point, as well as the values of the electric field and electron energy corresponding to this point.

$$w_c \approx -\frac{27}{64} - 11\left(\frac{2}{3}\right)^6\lambda^2 \approx -0.421875 - 0.965706\lambda^2 \tag{20}$$

$$p_c \approx \left(\frac{9}{8}\right)^3 + \frac{7\cdot 2^3\cdot 3^7\lambda^2}{3^{10}+2^{12}\cdot 11^2\lambda^2} = p_{c0} + \frac{7\cdot 2^3\cdot 3^7\lambda^2}{3^{10}+2^{12}\cdot 11^2\lambda^2} \tag{21}$$

$$f_c \approx \frac{2^{12}}{3^9} - \frac{5\cdot 2^{23}}{3^{17}}\lambda^2 = f_{c0} - \frac{15}{2}f_{c0}^2\lambda^2 \approx 0.208098 - 0.324787\lambda^2 \quad (22)$$

$$\varepsilon_c \approx -\frac{2^7}{3^5} + \frac{2^{20}}{3^{14}}\lambda^2 = \varepsilon_{c0} + \frac{3}{2}|\varepsilon_{c0}|^3\lambda^2 \approx -0.526749 + 0.219231\lambda^2 \quad (23)$$

For $\lambda = 0.25$, the accuracy of the approximation (compared to the numerical solution used here) in the case of f_c is 1.2% and in the case of ε_c is 0.2%, which shows that the approximation is good for the realistic values of λ.

From the approximation we see once again that the non-zero size of the internal system decreases the electric field, corresponding to the classical ionization threshold, and increases the energy and the orbit radius corresponding to it. We also note that Eq. (20) shows the maximum possible value of the induced electric dipole moment w_{max}: the allowance for the non-zero size of the internal system increases $|w_{max}|$ compared to its value at $\lambda = 0$.

3. CONCLUSIONS

For hydrogenic CRS studied in paper [11], the electric field caused the induced electric dipole moment (manifested by the shift of the circular orbit of the electron in the direction opposite to the applied field) and thus the quadratic Stark effect. Of course, there was no linear Stark effect because the unperturbed circular orbit of the electron did not have the electric dipole moment.

In the present paper we studied analytically how the difference of heliumic systems from hydrogenis systems – the difference due to the non-zero size of the inner subsystem (manifested by the non-zero value of the parameter λ defined in Eq. (11)) – affects the results. We found that increasing the size of the inner system (i.e., the parameter λ) decreases the electric field corresponding to the classical ionization threshold, and increases the energy and the orbit radius corresponding to it. Also, the allowance for the non-zero size of the internal subsystem increases the maximum possible absolute value of the induced electric dipole moment compared to its value at $\lambda = 0$.

References

1. E. Lee, D. Farrelly, T. Uzer, Optics Express **1**, 221 (1997)
2. T.C. Germann, D.R. Herschbach, M. Dunn, and D.K. Watson, Phys. Rev. Lett. **74**, 658 (1995)
3. C.H. Cheng, C.Y. Lee, and T.F. Gallagher, Phys. Rev. Lett. **73**, 3078 (1994)
4. L. Chen, M. Cheret, F. Roussel, and G. Spiess, J. Phys. B **26**, L437 (1993)
5. S.K. Dutta, D. Feldbaum, A. Walz-Flannigan, J.R. Guest, and G. Raithel, Phys. Rev. Lett. **86**, 3993 (2001)
6. R.G. Hulet, E.S. Hilfer, and D. Kleppner, Phys. Rev. Lett. **55**, 2137 (1985)
7. K.B. MacAdam and E. Horsdal-Petersen, J. Phys. B **36**, R167 (2003)
8. V.M. Vainberg, V.S. Popov, and A.V. Sergeev, Sov. Phys. JETP **71**, 470 (1990)
9. C.M. Bender, L.D. Mlodinow, and N. Papanicolaou, Phys. Rev. A **25**, 1305 (1982)
10. V.M. Vainberg, V.D. Mur, V.S. Popov, and A.V. Sergeev, Sov. Phys. JETP **66**, 258 (1987)
11. E. Oks, Europ. Phys. J. D **28**, 171 (2004)
12. Beletsky, V.V. Essays on the Motion of Celestial Bodies (Basel: Birkhäuser/Springer), 2001, Sect 1.7
13. E. Oks, New Astronomy **74**, 101301 (2020)